communications
earth & environment

ARTICLE

https://doi.org/10.1038/s43247-022-00474-x OPEN

The Angola Gyre is a hotspot of dinitrogen fixation in the South Atlantic Ocean

Tanya Marshall[1✉], Julie Granger[2], Karen L. Casciotti[3], Kirstin Dähnke[4], Kay-Christian Emeis[4,5], Dario Marconi[6], Matthew R. McIlvin[7], Abigail E. Noble[8,9], Mak A. Saito[8], Daniel M. Sigman[6] & Sarah E. Fawcett[1]

Biological dinitrogen fixation is the major source of new nitrogen to marine systems and thus essential to the ocean's biological pump. Constraining the distribution and global rate of dinitrogen fixation has proven challenging owing largely to uncertainty surrounding the controls thereon. Existing South Atlantic dinitrogen fixation rate estimates vary five-fold, with models attributing most dinitrogen fixation to the western basin. From hydrographic properties and nitrate isotope ratios, we show that the Angola Gyre in the eastern tropical South Atlantic supports the fixation of 1.4–5.4 Tg N.a^{-1}, 28-108% of the existing (highly uncertain) estimates for the basin. Our observations contradict model diagnoses, revealing a substantial input of newly-fixed nitrogen to the tropical eastern basin and no dinitrogen fixation west of 7.5°W. We propose that dinitrogen fixation in the South Atlantic occurs in hotspots controlled by the overlapping biogeography of excess phosphorus relative to nitrogen and bioavailable iron from margin sediments. Similar conditions may promote dinitrogen fixation in analogous ocean regions. Our analysis suggests that local iron availability causes the phosphorus-driven coupling of oceanic dinitrogen fixation to nitrogen loss to vary on a regional basis.

[1] Department of Oceanography, University of Cape Town, Cape Town 7708, South Africa. [2] Department of Marine Sciences, University of Connecticut, Groton, CT 06340, USA. [3] Department of Earth System Science, Stanford University, Stanford, CA 94305, USA. [4] Helmholtz-Zentrum Hereon, Institute of Carbon Cycles, 21502 Geesthacht, Germany. [5] Institute of Geology, Universität Hamburg, Hamburg 20146, Germany. [6] Department of Geosciences, Princeton University, Princeton, NJ 08544, USA. [7] Schmidt Ocean Institute, Palo Alto, CA 94301, USA. [8] Department of Marine Science and Geochemistry, Woods Hole Oceanographic Institution, Woods Hole, MA 02540, USA. [9] California Department of Toxic Substances Control, Sacramento, CA 95814, USA. ✉email: mrstan001@myuct.ac.za

The cycling of nitrogen (N) controls the fertility of the global ocean[1,2] and may influence the ocean's role in climate[3]. The ultimate source of marine N to the ocean is N_2 fixation, whereby specialized plankton, diazotrophs, transform inert N_2 gas into bioavailable ammonium. This process occurs dominantly in the warm, sunlit surface of the (sub)tropical ocean. The ultimate sink for marine N is denitrification, the bacterial reduction of oxidized N species to N_2 gas in oxygen-deficient waters and sediments. Considerable uncertainty exists regarding the magnitude of the global N source and sink terms, including whether these are balanced on timescales of ocean mixing[4–7]. An incomplete understanding of the controls on N_2 fixation, particularly at the regional scale, likely contributes to the apparent discrepancies in estimates of oceanic N loss and gain.

A stoichiometric phosphorus (P) excess relative to N, termed 'excess P', is a condition proposed to favour N_2 fixation[6]. Much of the global surface ocean hosts excess P[8], which ultimately derives from denitrification in oxygen-deficient zones and sediments[6,9]. The South Atlantic receives excess P both remotely and regionally, in the latter case following seasonal N loss in the northern Benguela upwelling system (NBUS)[6,10,11], yet this basin appears to support little N_2 fixation. Direct and geochemical estimates of South Atlantic N_2 fixation rates, although notably sparse, range from 1.8 to 8.4 Tg N.a^{-1}, with disagreement as to the regional distribution[6,12–17] (Table 1). These low rates have been attributed to iron limitation of diazotrophs[9,14,17–19] as the South Atlantic receives at least a hundred-times less aeolian iron than the North Atlantic (3 ± 2 versus 896 ± 14 nmol iron.m^{-2}.d^{-1})[20] where N_2 fixation is considerably higher, with estimates ranging from 24 to 47 Tg N.a^{-1} [6,9,12–16,21] (Table S1). The excess P that goes largely unused in the South Atlantic traverses the basin in its equatorward-flowing surface layer, ultimately fuelling N_2 fixation in the (sub)tropical North Atlantic following its entrainment into iron-replete, P-limited surface waters[9,14,22]. Nevertheless, some N_2 fixation likely occurs in the South Atlantic, yet its magnitude and distribution, and the controls thereon, remain poorly characterized.

The estimation of N_2 fixation has often relied on ocean models, most of which exploit regional variations in the nitrate-to-phosphate (NO_3^-:PO_4^{3-}) ratio[6,12,13] to derive rates from inverse circulation fields. Variations in N:P are typically quantified by the parameters N* and P*[6,23,24], defined here as $[NO_3^-] - 15.5 \times [PO_4^{3-}]$[23] and $[PO_4^{3-}] - [NO_3^-]/15.5$[6], respectively, where 15.5:1 is the mean N:P ratio of nutrients supplied to the tropical South Atlantic thermocline (SI.1). The conceptual basis for the estimation is that diazotrophy pairs the production of newly-fixed N with the assimilation of P. N_2 fixation thus removes P but not N from surface waters and leads to a sinking organic matter (OM) flux with an N:P ratio that is higher than that of the net supply of nitrate and phosphate to the surface[6,23,25]. However, the N:P ratio of plankton biomass, and thus of sinking OM, varies regionally[26], complicating the calculation of N_2 fixation rates based on nutrient stoichiometry[27]. Recent modelling efforts have attempted to address this shortcoming by including variable, yet still prescribed, OM N:P ratios[13].

Nitrate isotope ratio measurements provide an important alternative source of information for diagnosing N_2 fixation[14,28,29]. N_2 fixation introduces nitrate to the thermocline with a $\delta^{15}N$ of −2 to 0‰[28,30–32], distinct from that of deep-ocean nitrate (≥5‰[33]; $\delta^{15}N = [(^{15}N/^{14}N)_{sample}/(^{15}N/^{14}N)_{ref} - 1] \times 10^3$, in ‰ versus N_2 in the air). Negative excursions in source-to-thermocline nitrate $\delta^{15}N$ can thus be used to diagnose and quantify N_2 fixation[28]. The N isotope ratios have some major advantages over N:P ratios in this regard. In particular, the $\delta^{15}N$ of newly-fixed N is relatively well-constrained[30,31], whereas the N:P ratios of both diazotrophs and non-N_2-fixing plankton are uncertain and potentially dynamic[25–27].

Here we analyse nitrate isotope ratios and nutrient stoichiometries for the tropical South Atlantic Ocean based on new and existing measurements[14,34–36] (see 'Methods'). These data reveal substantial N_2 fixation in the Angola Gyre to the east of the basin and none in the west, in contrast to current notions that N_2 fixation occurs predominantly in the western tropical South Atlantic[6,13] (Fig. 1). We hypothesize that the confluence of remote and regional sources of excess P and iron supplied proximately from the ocean margin determines the incidence of N_2 fixation in the Angola Gyre. Our findings have implications for regional variations in N_2 fixation and its coupling to N loss throughout the global ocean[37,38].

Results and discussion

Properties of the Angola Gyre. The Angola Gyre, a permanent upwelling feature embedded within the larger-scale cyclonic South Atlantic Tropical Gyre[39–41], was encountered east of 7.5°W along a zonal transect of the Atlantic at 6-15°S (Fig. 1; CoFeMUG[14,34] and MET131 cruises; see 'Methods'). The gyre is characterized by a shoaling of the thermocline, defined as the waters between potential density anomalies (σ_θ; in kg.m^{-3}) 26.2 and 27.0, overlying an oxygen minimum zone where apparent oxygen utilization ($AOU = O_{2saturated} - O_{2observed}$) is >240 μM[40–42] (Fig. 2a, b, f, g). High rates of primary productivity fuelled by persistent nutrient upwelling drive elevated OM export from the Angola Gyre mixed layer, which is remineralized in the aphotic zone below the surface[43,44]. A subsurface iron plume emanating from the nearby low-oxygen marginal sediments penetrates the Angola Gyre (dFe ~0.8–2 nM; Fig. 2c). Intense remineralization and repeated cycles of supply and export retain this bioavailable iron within Angola Gyre waters[34]. Local remineralization also yields a

Table 1 Existing areal N_2 fixation rate estimates (Tg N.a^{-1}) for the South Atlantic.

Domain	Method	Rate [Tg N.a^{-1}]	Reference
0°S–25°S	N* plus forward circulation model	8.4	12
11°S–35°S	N:P plus inverse circulation model	8.3	13
0°S–40°S	P* plus inverse circulation model	7.5[a]	6
11°S–30°S	Nitrate isotopes plus volume flux	3 ± 0.5	14
10°S–45°S	Direct rate measurements	5 ± 2[b]	15
0°S–40°S	Direct rate measurements	1.8 ± 0.6[b]	16
6°S–15°S	Nitrate isotopes plus residence time	2.0-4.1	This study

The arithmetic mean (±1 SD) for 5°S to 35°S is 5.0 ± 3.3 Tg N.a^{-1}. This average excludes our N_2 fixation estimate, which is relevant to the tropical South Atlantic domain only. For a detailed list of the available areal N_2 fixation rate estimates, see Table S1.
[a]Estimated from a homogenized rate for the South Atlantic (area = 27 × 10^{12} m^2 for 0–40°S[16]).
[b]Compilation of direct measurements made by others.

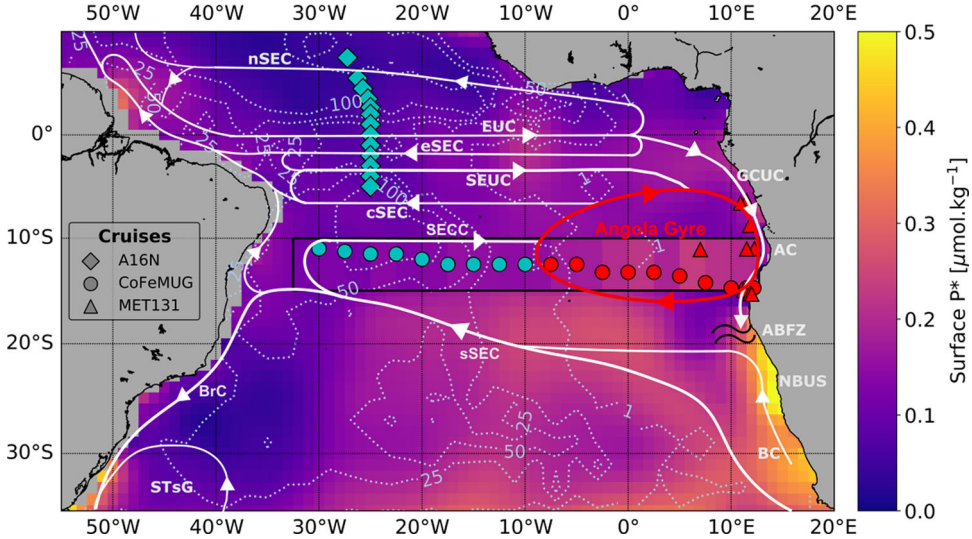

Fig. 1 Surface P* across the South Atlantic Ocean. Station locations (coloured symbols) overlaid on an annual climatology of the South Atlantic surface P* concentration (=[PO_4^{3-}]-[NO_3^-]/15.5; SI.1). As indicated in the legend, circles represent stations sampled during the CoFeMUG cruise in November/December 2007[14,34], triangles show stations sampled during the MET131 cruise in October 2016, and diamonds indicate stations sampled during the CLIVAR/GO-SHIP A16N cruise in September/October 2013[14,49]. Red symbols show Angola Gyre stations and blue symbols represent western basin stations. The red cell indicates the approximate position of the Angola Gyre, and the white arrows show the circulation of thermocline waters in the tropical South Atlantic Ocean. The black box encloses P* values calculated from the CoFeMUG data set, while the other P* data are from WOA18[8] (SI.1). The dotted light-grey contours show the distribution of recent modelled water column-integrated N_2 fixation rates for the South Atlantic(1, 25, 50 and 100 mmol N.m^{-2}.a^{-1})[13]. The South Atlantic Tropical Gyre is defined by the sSEC, SEUC and AC, where sSEC is south South Equatorial Current, SEUC is South Equatorial Undercurrent, and AC is Angola Current. Additionally, nSEC is north South Equatorial Current, EUC is Equatorial Undercurrent, eSEC is equatorial South Equatorial Current, cSEC is central South Equatorial Current, SECC is South Equatorial Countercurrent, GCUC is Gabon-Congo Undercurrent, ABFZ is Angola-Benguela Frontal Zone (indicated by the parallel wavy lines), NBUS is northern Benguela upwelling system, BC is Benguela Current, BrC is Brazil Current, and STsG is Subtropical subgyre.

nitrate concentration maximum (>40 μM) beneath the thermocline ($\sigma_\theta > 27.0$), contrasting with the lower concentration of sub-thermocline nitrate (<35 μM) and AOU (<180 μM) in the tropical western basin (west of 7.5°W; Figs. 2b, g and 3a).

Nitrate $\delta^{15}N$ across the transect is consistently high in Tropical Surface Water ($\sigma_\theta < 26.2$) due to isotopic fractionation during nitrate assimilation by phytoplankton, which raises nitrate $\delta^{15}N$ (and $\delta^{18}O$[45,46]; which, in ‰ versus VSMOW = $[(^{18}O/^{16}O)_{sample}/(^{18}O/^{16}O)_{ref} - 1] \times 10^3$; SI.3) to >12‰. The mean nitrate $\delta^{15}N$ in the underlying thermocline is 5.7 ± 0.7‰ in the Angola Gyre, reaching as low as 4.6‰, a salient decrease from the western tropical basin where the average $\delta^{15}N$ of thermocline nitrate is 6.3 ± 0.1‰ (Figs. 2d, h and 3b). Subantarctic Mode Water (SAMW; σ_θ = 27.0–27.25), recently formed in the Southern Ocean, underlies the thermocline of the tropical South Atlantic and is the ultimate source of nutrients to its surface waters[47]. In the western tropical basin, SAMW nitrate $\delta^{15}N$ is 6.2 ± 0.1‰, indistinguishable from the $\delta^{15}N$ of SAMW nitrate beneath the Angola Gyre (6.4 ± 0.1‰; $t(150) = -12.05$, $p = 0.01$) (Figs. 2d, h and 3b).

Mean SAMW N* is 0.0 ± 0.1 μM across the basin, increasing in the Angola Gyre thermocline to 0.7 ± 0.9 μM, coincident with the source-to-thermocline decline in nitrate $\delta^{15}N$. N* decreases into the western tropical basin thermocline, to −0.4 ± 0.5 μM (Fig. 3c and SI.1 and 4).

Zonal trends in the tropical South Atlantic: evidence for an exogenous source of N to the Angola Gyre. Thermocline nitrate $\delta^{15}N$ in the western tropical South Atlantic basin is similar to that of the underlying source (6.3 ± 0.1‰ versus 6.2 ± 0.1‰) while the $\delta^{15}N$ of nitrate in the Angola Gyre thermocline is distinctly lower, by 0.7–1.8‰ (Figs. 2d, h and 3b). Since surface-water nitrate is generally completely consumed, and given that nitrification in the ocean interior typically competes with no other process—thus negating the impact of isotopic fractionation during remineralization in the subsurface—remineralized OM produced from Tropical Surface Water will return nitrate to the thermocline with a $\delta^{15}N$ that is indistinguishable from the underlying SAMW source[29,48,49]. The fact that the $\delta^{15}N$ of thermocline nitrate in the Angola Gyre is lower than SAMW nitrate $\delta^{15}N$ signals an exogenous source of N to surface waters, the consumption and subsequent remineralization of which yields low-$\delta^{15}N$ nitrate in the Angola Gyre thermocline[28,32].

Zonal and vertical changes in nutrient stoichiometry corroborate the notion of an exogenous source of N to the Angola Gyre. The SAMW-to-thermocline N* increase in the gyre is consistent with the addition of N in stoichiometric excess of P (i.e., relative to the N:P ratio of the regional nutrient supply, 15.5:1) while the SAMW-to-thermocline N* decrease in the western tropical basin suggests that sinking OM may be lower in N:P than the regional nutrient supply (SI.4).

Despite the existing data pointing to complete nitrate consumption in the Angola Gyre surface, instances of incomplete nitrate assimilation could occur in this perennially-upwelling feature, and these could cause the loss of high-$\delta^{15}N$ nitrate (by advection), with low-$\delta^{15}N$ OM retained and remineralized in the gyre thermocline[29,50]. However, the regeneration of OM deriving from partial nitrate assimilation, which would have an N:P of ~15.5:1, could not yield the high N* observed in the thermocline. Additionally, mixed-layer nitrate was measurable at only three of 19 stations at the time of our sampling, reinforcing the view that nitrate is seldom unconsumed in Angola Gyre surface waters in spring, and likewise in autumn[44]. The $\delta^{15}N$ of thermocline nitrate could arguably be lowered by the lateral export of high-$\delta^{15}N$ dissolved organic N from the gyre surface. However, high-$\delta^{15}N$ dissolved organic N export cannot account for the regional increase in thermocline N*. We thus rule out partial nitrate

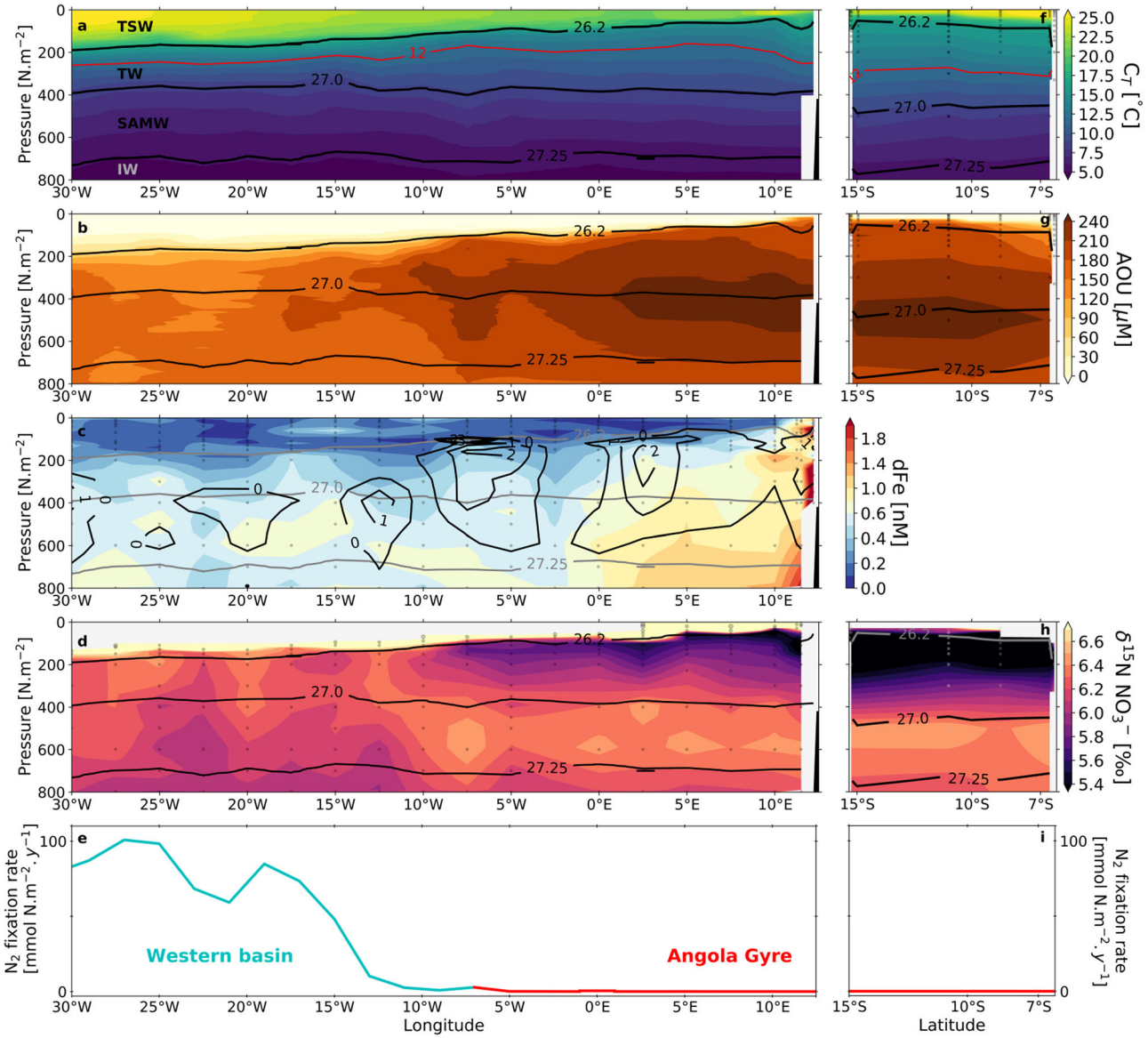

Fig. 2 Zonal trends in physical and biogeochemical properties across the tropical South Atlantic. Gridded section plots across the CoFeMUG (30°W to 12°E; **a**–**d**) and MET131 (6°S to 15.1°S; **f**–**h**) transects of **a**, **f** conservative temperature in °C, where the red contour denotes the 12 °C isotherm, the shoaling of which between 7.5°W and 12.2°E marks the approximate zonal extent of the Angola Gyre[40]; **b**, **g** apparent oxygen utilization (AOU) in μM; **c** dissolved iron concentrations in nM[34] overlaid by N* contours (black) in μM; and **d**, **h** nitrate $\delta^{15}N$ in ‰ versus N_2 in the air (CoFeMUG data from ref. [14]). **e**, **i** shows a recent modelled water column-integrated N_2 fixation rate along 11°S (**e**) and 11°E (**i**) in mmol N.m^{-2}.a^{-1} [13], with the western basin values in blue and the Angola Gyre values in red. Black (grey) contours on **a**, **b**, **d**, **f**, **g**, **h** (**e** and **h**) are potential density surfaces indicating tropical water masses, where TSW is Tropical Surface Water, TW is Thermocline Water, SAMW is Subantarctic Mode Water and IW is Intermediate Water (SI.2). Small grey circles in **c**, **d** and **h** indicate the sampling resolution.

assimilation and dissolved organic N export as explanations for the low $\delta^{15}N$ of Angola Gyre thermocline nitrate.

Atmospheric deposition can introduce exogenous N to the surface ocean with a $\delta^{15}N < 0‰$[51] and an N:P ratio >1000:1[52], potentially explaining both the low-$\delta^{15}N$ nitrate and high N* of the Angola Gyre thermocline. However, estimates of the N deposition flux to the South Atlantic are orders of magnitude too low to account for our observations[52] (SI.5). We thus conclude that the exogenous N in the Angola Gyre thermocline derives from N_2 fixation.

Origin of the N_2 fixation signal in the Angola Gyre thermocline. The low $\delta^{15}N$ of Angola Gyre thermocline nitrate could originate, at least partly, in the tropical North Atlantic basin where N_2 fixation rates are elevated[14,17,28,49], and be transported into the gyre by equatorial feeder currents (Fig. 1). We address this possibility by estimating the concentration-weighted influx of nitrate $\delta^{15}N$ by the three Angola Gyre feeder currents: the Equatorial Undercurrent, the South Equatorial Undercurrent, and the South Equatorial Countercurrent[40]. We estimate the $\delta^{15}N$ of the Equatorial Undercurrent, South Equatorial Undercurrent, and South Equatorial Countercurrent end-members to be 5.7‰, 6.0‰, and 6.3‰, respectively ('Methods'; SI.6). The relative contribution of each current to Angola Gyre thermocline nitrate based on transport volumes[42] yields a mean flux-weighted nitrate-$\delta^{15}N$ of 6.1 ± 0.1‰. While lower than the $\delta^{15}N$ of underlying SAMW (6.4‰), this end-member is not low enough

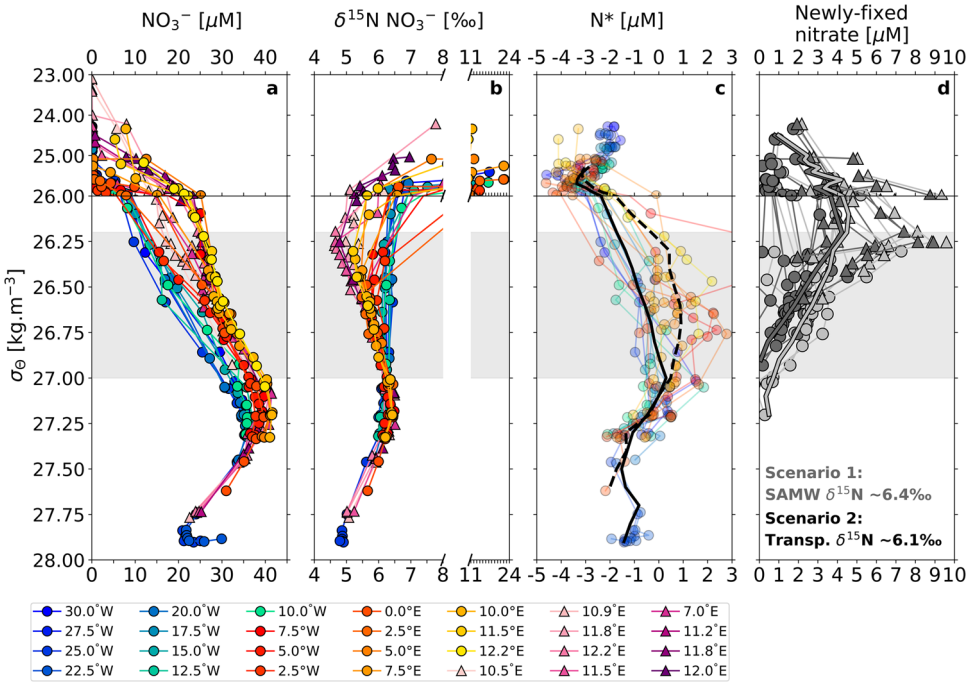

Fig. 3 Characteristics of tropical South Atlantic nitrate. Density profiles of **a** nitrate concentrations in μM; **b** nitrate $\delta^{15}N$ in ‰ versus N_2 in air; **c** N* (= $[NO_3^-] - 15.5 \times [PO_4^{3-}]$; SI.1) in μM; and **d** the depth-specific concentration of newly-fixed nitrate in μM in the Angola Gyre. In **a**–**c**, warm (cool) coloured profiles represent stations from the Angola Gyre (tropical western basin). Round markers show data from the CoFeMUG transect while triangle markers represent data from the MET131 transect. The legend provides station longitude. The grey shading on **a**–**d** indicates the density range of TW. In c, the dashed (solid) black line indicates the mean gridded N* for the Angola Gyre (western basin) stations; only CoFeMUG data are shown here because of the higher depth resolution of this sample set. **d** shows the concentration of newly-fixed nitrate in the Angola Gyre, computed by multiplying the depth-specific fraction of newly fixed nitrate ($f_{depth_specific}$; equation S3b) by the corresponding nitrate concentration at each depth. To calculate $f_{depth_specific}$, a nitrate $\delta^{18}O$-based correction is applied to the $\delta^{15}N$ data to remove the phytoplankton nitrate assimilation signal from Tropical Surface Water (SI.7). Light grey data show results from scenario 1 while dark grey data show scenario 2 (see text for details). The mean of each scenario is indicated by the bold line of corresponding colour.

to decrease Angola Gyre thermocline nitrate $\delta^{15}N$ to 5.7‰ (nor to the observed minimum of 4.6‰). Thus, some amount of the low-$\delta^{15}N$ signal must derive from local N_2 fixation.

Our conclusion that N_2 fixation occurs in the Angola Gyre is further supported by the slightly lower $\delta^{15}N$ of nitrate at the depth of the AOU maximum compared to that of core SAMW (6.2‰ versus 6.4‰; Fig. 2b, g, d, h). Given that the provenance of the high AOU signal is in situ primary production[40], OM remineralized at the AOU maximum is lower in $\delta^{15}N$ than SAMW nitrate, consistent with its low $\delta^{15}N$ deriving from N_2 fixation in Angola Gyre surface waters. Additional support comes from direct rate measurements made during the CoFeMUG cruise[53] and other rate data from near the Angola Gyre[15,54,55], which indicate N_2 fixation rates ranging from undetectable to ~170 μmol $N.m^{-2}.d^{-1}$. Regional observations of diazotrophs (*Trichodesmium* spp. being the most abundant) and diatoms hosting N_2-fixing symbionts (*Rhizosolenia* and *Chaetoceros* spp.) further substantiate the occurrence of N_2 fixation in the Angola Gyre[53,54,56,57].

Quantifying the N_2 fixation rate in the Angola Gyre. Using our nitrate $\delta^{15}N$ data, we estimate the annual rate of N_2 fixation in the Angola Gyre, considering two scenarios: (1) the low-$\delta^{15}N$ of thermocline nitrate is generated solely from in situ N_2 fixation and superimposed on SAMW nitrate, and (2) local N_2 fixation contributes the fraction of low-$\delta^{15}N$ thermocline nitrate that is not supplied by the equatorial feeder currents. For both scenarios, we estimate the fraction (f) of newly fixed nitrate in the Angola Gyre as:

$$f = \frac{\delta^{15}N_{AGmean} - \delta^{15}N_{scenario_mean}}{\delta^{15}N_{N_2fix} - \delta^{15}N_{scenario_mean}} \quad (1)$$

$\delta^{15}N_{AGmean}$ is the mean concentration-weighted $\delta^{15}N$ of Angola Gyre nitrate for the upper water column ($\sigma_\theta \leq 27.0$), estimated to be 5.7 ± 0.4‰ (5.5–5.9‰; 5th−95th percentiles; Methods), $\delta^{15}N_{N2fix}$ is the $\delta^{15}N$ of nitrate regenerated from diazotrophic OM, −1‰[30,31], and $\delta^{15}N_{scenario_mean}$ is the scenario-specific mean concentration-weighted $\delta^{15}N$ of nitrate supplied to the Angola Gyre thermocline (6.4 ± 0.1‰ and 6.1 ± 0.1‰ for scenarios 1 and 2, respectively).

For scenario 1, $f = 9\%$ (6–12%; 5th−95th percentiles) and for scenario 2, $f = 6\%$ (2–9%; 5th−95th percentiles). On average, therefore, 6–9% (associated with scenarios 2 and 1, respectively) of the nitrate above SAMW originates from local N_2 fixation. This mass-balance method neglects particulate organic N, which is reasonable given that this pool contributes negligibly to total N, accounting for <1% of the fixed N reservoir above $\sigma_\theta = 27.0$. Our approach is validated by the concentration-weighted $\delta^{15}N$ that it yields for nitrate above $\sigma_\theta = 27.0$ in the western tropical basin of 6.3 ± 0.1‰ (6.2–6.4‰; 5th−95th percentiles), indistinguishable from that of SAMW (6.2 ± 0.1‰). This correspondence further confirms that N_2 fixation is negligible in the tropical waters west of the Angola Gyre.

To visualize the depth distribution of newly-fixed nitrate in the Angola Gyre, we calculate $f_{depth_specific}$ (i.e., the fraction of the

nitrate pool at each depth that is newly fixed) for each sample above $\sigma_\theta = 27.0$, after removing the signal of phytoplankton assimilation from nitrate $\delta^{15}N$ using the coincident nitrate $\delta^{18}O$ data ('Methods'; SI.7). This exercise reveals that a substantial fraction of Tropical Surface Water nitrate is newly-fixed, which is not apparent from the nitrate $\delta^{15}N$ profiles because fractionation during nitrate assimilation overprints the isotopic signal of newly nitrified N (Fig. 3b, d). It is not appropriate, however, to integrate these depth-specific estimates to yield a measure of the newly-fixed N inventory. This is due to the likelihood of 'double-counting'—that is, low-$\delta^{15}N$ nitrate assimilated in the surface is returned to the thermocline when the resulting OM is exported and remineralized, such that at the scale of the water column, correction of shallow nitrate-$\delta^{15}N$ for nitrate assimilation is unnecessary[28]. Instead, the mass-balance approach represented by Eq. 1 is most appropriate for estimating the water column burden of newly fixed N.

Multiplying f (Eq. 1) by the mean Angola Gyre nitrate concentration for $\sigma_\theta \leq 27.0$ indicates that local N_2 fixation supplies 313–641 mmol N.m^{-2} to the thermocline nitrate reservoir. The residence time of thermocline waters in the Angola Gyre is 4.4–8.5 years[40] and its areal extent is 2.6×10^{12} m^2. These constraints yield an N_2 fixation rate of 2.8-5.4 Tg N.a^{-1} (mean of 4.1 ± 2.8 Tg N.a^{-1}) for scenario 1 and 1.4-2.6 Tg N.a^{-1} (mean of 2.0 ± 3.0 Tg N.a^{-1}) for scenario 2, considering both extrema for residence time ('Methods'; SI.8). Our estimates are equivalent to daily rates of 102–390 μmol N.m^{-2}.d^{-1}, comparable to incubation-based N_2 fixation rates measured near the Angola Gyre[15,53–55] (SI.9).

The Angola Gyre is a hotspot for N_2 fixation in the South Atlantic. Our N_2 fixation rate estimates imply that the Angola Gyre accounts for 28–108% of the highly uncertain mean South Atlantic N_2 fixation rate of 5.0 ± 3.3 Tg N.a^{-1} (Table 1). Since the latter derives from few observations that are sparsely distributed across the basin, it would be unwise to conclude that the Angola Gyre makes a disproportionate contribution to South Atlantic N_2 fixation. Nonetheless, since the Angola Gyre occupies only ~10% of the South Atlantic by area, our data indicate that it is a hotspot for N_2 fixation. Conditions particular to the Angola Gyre must render this feature favourable for N_2 fixation.

The phosphate-bearing, nitrate-deplete surface waters of the South Atlantic receive a limited supply of aeolian iron[20], a condition proposed to limit N_2 fixation across the basin[9,13,14,17,38]. The non-aeolian iron supply to the Angola Gyre must thus be substantial. The Congo-shelf-zone near the Angola Gyre has been reported to supply a substantive quantity of iron to the marginal ocean, equivalent to 40 ± 15% of the entire South Atlantic aeolian iron flux[58], and the elevated iron concentrations observed in the vicinity of the Angola Gyre (Fig. 2c) are evidence of this sedimentary iron supply. We hypothesize that the subsurface iron plume, which is trapped by the retentive regional circulation of the Angola Gyre through repeated cycles of upward supply, export, and remineralization[34], relieves diazotrophs in the overlying surface waters of iron limitation.

We thus conclude that N_2 fixation occurs in the Angola Gyre because of the overlapping biogeography of excess P and bioavailable iron. While the iron supply to the Angola Gyre is local, originating from the nearby low-oxygen margin sediments, the excess P derives from both regional and remote N loss. The apparent importance of margin-derived iron echoes a growing body of work showing that sedimentary iron sources are important to the global ocean iron budget[59–62]. The notion that both iron and excess P together limit N_2 fixation at the regional scale in the South Atlantic is compatible with previous work showing negligible rates of N_2 fixation in the western tropical basin where measurements were made in P-bearing but iron-limited waters[9,17,22].

The possibility of additional N_2 fixation hotspots. We hypothesize that N_2 fixation hotspots are inherent to ocean regions characterized by biogeochemical conditions analogous to those encountered in the Angola Gyre, possibly enhanced by retentive circulation features (SI.10). In the subtropical South Atlantic where the Brazil Current recirculation forms a subgyre adjacent to the continental shelf[41] (Fig. 1), an N_2 fixation hotspot should result as waters bearing a remote (i.e., Southern Ocean-derived) and regional (i.e., NBUS-derived) supply of excess P[6] (Fig. 1) encounter a local supply of sediment-derived iron[62]. Observations of diazotroph blooms[63] and low-$\delta^{15}N$ thermocline nitrate[64] in the Brazil subgyre validate this prediction. In addition, the cyclonic Guinea Dome in the eastern tropical North Atlantic receives excess P from local upwelling of P-rich subsurface waters[8] and iron from dust deposition, possibly augmented by an iron flux from the nearby low-oxygen margin sediments[60]. Direct N_2 fixation rate measurements[15,16], the presence of diazotrophs[16,65], and low-$\delta^{15}N$ thermocline nitrate[66] in the vicinity of the Guinea Dome are consistent with this region also being an N_2 fixation hotspot.

The surface waters above or just offshore of the ocean's major suboxic zones would, in general, appear well-suited to host hotspots of N_2 fixation. Denitrification in both the shallow subsurface water column and the adjacent sediments generates an N deficit (i.e., a P excess)[6]. At the same time, the adjacency of these zones to low-oxygen margin sediments, coupled with water column suboxia overlying some of the sediments, supplies iron to the water column[59,67,68]. These regions are also characterized by upwelling, which would transport both the excess P and the iron into the surface mixed layer. In these surface waters or just offshore, phytoplankton assimilation leaves nitrate-free but P- and iron-bearing surface waters[6,67–69], a seemingly ideal recipe for N_2 fixation.

However, the existing data are ambiguous as to the rates of N_2 fixation above and nearby the suboxic zones. Observations from the Arabian Sea support elevated N_2 fixation[70–72] while incubation-based measurements in the eastern tropical Pacific suggest negligible to extremely high rates[38,73–78]. Notably, incubation experiments suggest that N_2 fixation occurs in the Costa Rica Dome[75], a retentive feature embedded within the eastern tropical Pacific suboxic zone that is characterized by similar hydrography to the Angola Gyre. In the water column of all the suboxic zones, a decrease in nitrate $\delta^{15}N$ is observed above the very high nitrate $\delta^{15}N$ associated with denitrification[79–82]; this upward $\delta^{15}N$ decline has been interpreted as evidence of local N_2 fixation[79]. Additionally coupled nitrate $\delta^{15}N$ and $\delta^{18}O$ measurements from the eastern tropical North Pacific indicated a lower nitrate $\delta^{15}N$ than is expected from nitrate $\delta^{18}O$ in the upper portion of the suboxic zone, also consistent with a role for N_2 fixation[80]. However, N cycling processes occurring within suboxic waters (e.g., nitrite oxidation) provide an alternative explanation for the observed $\delta^{15}N$-$\delta^{18}O$ decoupling[80–84], complicating the use of the nitrate isotopes to evaluate N_2 fixation above and near the major suboxic zones. Importantly, the Angola Gyre is not complicated by the same suboxic zone N cycling processes, allowing us to pinpoint the role of N_2 fixation in this system. Our findings for the Angola Gyre thus suggest that the nitrate $\delta^{15}N$ decline in the shallow subsurface of the suboxic zones may have a similar origin. The nitrate isotope data of the major ocean suboxic zones should be revisited with this new perspective.

Implications of regional N_2 fixation hotspots. N_2 fixation has been proposed to be spatially and/or quantitatively coupled to N loss at the basin scale[6,10,85]. Our estimate of N_2 fixation in the Angola Gyre is notably comparable to N loss from the NBUS (1.4–2.5 Tg N.a^{-1})[11,86]. In this regard, the generation and advection of excess-P waters from the NBUS have been hypothesized to fuel N_2 fixation in the vicinity of the Angola Gyre[10], prompting the suggestion that N sources and sinks in the south-eastern Atlantic are coupled. However, surface P* is perennially elevated across the (sub)tropical South Atlantic, including in Angola Gyre and Brazil subgyre surface waters[6,9] (Fig. 1). Accordingly, it is not clear that the additional flux of excess P from the NBUS, by itself, stimulates N_2 fixation in the Angola Gyre. Rather, N_2 fixation would likely occur in the Angola Gyre regardless of whether it receives excess P from the NBUS, provided that the iron supply is sustained. That is, the greatest influence of the NBUS on N_2 fixation in the Angola Gyre may be through its augmentation of the iron supply. In summary, our findings argue that a P-driven coupling of N_2 fixation to denitrification is contingent on a supply of iron, which is most easily achieved along coastal suboxic zones[59].

Because the South Atlantic hosts a basin-wide surface P excess, a future increase in the iron supply to the south-eastern Atlantic due to expanding low-oxygen margins[34,62,87] and/or a climate change-driven increase in aeolian deposition[88] could enhance N_2 fixation in and beyond the Angola Gyre. Consequently, the meridional flux of excess P across the Atlantic could decrease, engendering a shift in the dominance of N_2 fixation from the North to the South Atlantic.

Lessons for estimating basin-scale N_2 fixation rates. Our observations contradict diagnoses of the regional distribution of N_2 fixation in the South Atlantic computed from nutrient climatologies and velocity fields from ocean general circulation models[6,13] (e.g., P* convergence). This inconsistency highlights the current inadequacy of nutrient fields to deliver regional representations of N_2 fixation. Modelled distributions suggest that N_2 fixation predominantly occurs in the western and central tropical South Atlantic at a rate of 7.5-8.3 Tg N.a^{-1}, yet the nitrate-δ^{15}N data from these longitudes bear no evidence of the remineralization of low-δ^{15}N, diazotroph-derived OM (Figs. 2d and 3b). Thus, while the model diagnoses offer a powerful framework from which to estimate basin-scale N_2 fixation rates and conceptualize the global drivers thereof[6], some of the fundamental assumptions inherent to this approach can lead to erroneous diagnoses, potentially underpinning the discrepancy between our observations and existing model solutions. First, coarse resolution (2–4°) general circulation models used to simulate current velocities and transports typically resolve only gross circulation features. Although this limitation is widely acknowledged[6,12,13], the implications for estimates of N_2 fixation rates and distributions may be important, particularly at the regional scale. In particular, such general circulation models are unable to reliably simulate ocean-margin environments[12,37,61]. Second, the available South Atlantic nutrient climatologies include few data, particularly in the central basin, such that the choice of data set can considerably alter the modelled regional distribution of N_2 fixation[6]. Third, diagnoses of N_2 fixation from inverse models are highly sensitive to the N:P ratios of plankton biomass and exported OM. These properties are difficult to measure and are thought to be dynamic and sensitive to environmental conditions[25–27,89]. Elemental ratios of OM are thus typically parameterized[6,13] and may not accurately capture the plasticity of OM stoichiometry. Fourth, to parameterize dissolved OM in models, its production and degradation rates also have to be prescribed. However, few measurements of such rates exist—particularly with respect to dissolved organic phosphorus, which diazotrophs can assimilate when ambient phosphate concentrations are low[90,91]—resulting in modelled dissolved OM dynamics that are poorly constrained and potentially erroneous[92]. Finally, the analytical limit of quantification for [PO_4^{3-}] and [NO_3^-] is such that the propagated error on P* is ≥0.1 μM[93] (SI.11). Interpretations of ≤0.1 μM differences in P* may thus inaccurately diagnose the rate and/or distribution of N_2 fixation[94].

Pending enhanced observational coverage and improved model simulations of margin environments, convergent N_2 fixation distributions for the South Atlantic and other dynamic ocean-margin regions will remain elusive. Our work highlights the utility of nitrate isotope ratios for identifying and estimating N_2 fixation, and underscores the importance of regional observations, which are necessary for understanding the regional controls on N_2 fixation that ultimately determine its global distribution.

Materials and methods

Sample and data provenance. The CoFeMUG nutrient and nitrate isotope data were first published in refs. [34,14], respectively. Samples from the CoFeMUG cruise were collected onboard the R/V *Knorr* in November and December 2007 (Fig. 1). Seawater samples were measured for nitrate isotopes at the Woods Hole Oceanographic Institution using the denitrifier method[95,96]. Nitrate concentration and isotope data were first published from the CLIVAR A16N cruise in refs. [49,66]. The samples were collected onboard the NOAA R/V *Ronald H. Brown* between August and October 2013 as part of the GO-SHIP and CLIVAR program. The shipboard-ADCP data from this cruise are provided in Firing & Hummon (2010)[97]. The MET131 cruise data have not been previously published. This cruise was undertaken onboard the R/V *Meteor* in October 2016, with nine stations sampled between 6°S–15°S and 7°E–12°E. Twenty-four 12 L Niskin bottles attached to a Sea-Bird rosette with conductivity–temperature–depth (CTD) and oxygen sensors were remotely fired over the upper 1000 m to collect seawater samples for nutrient and nitrate isotope analysis. Samples were collected in thoroughly rinsed 30 ml HDPE bottles, filtered (0.4 μm), and immediately frozen at −20 °C until analysis.

Analysis of MET131 cruise nutrient concentrations and nitrate isotopes. Nitrate and phosphate concentrations ([NO_3^-], [PO_4^{3-}]) and the dual isotopes of nitrate were analysed at the Helmholtz–Zentrum Hereon in Germany. The concentrations of PO_4^{3-}, nitrite ([NO_2^-]) and nitrate plus nitrite ([NO_3^-] + [NO_2^-]) were measured colourimetrically using an automated continuous flow system (AA3, Seal Analytical, Germany) with a detection limit of 0.01 μM[98]; [NO_3^-] was then determined by subtraction. The dual isotopes of nitrate, following nitrite removal[99], were measured using the denitrifier method[95,96] whereby nitrate is quantitatively converted to nitrous oxide gas (N_2O) by denitrifying bacteria that lack an N_2O reductase enzyme. The N and O isotope ratios of the N_2O were measured using a Thermo Delta Plus XP isotope ratio mass spectrometer in-line with a GasBench II. The international reference materials, IAEA-N3[100] and USGS-34[101], were included in each run to enable post-run calibration of the N_2O measurements to N_2 in the air (δ^{15}N) and VSMOW (δ^{18}O). The standard deviation of duplicate measurements of δ^{15}N and δ^{18}O was <0.2‰ and <0.4‰, respectively.

Data gridding and interpolation. The CoFeMUG and MET131 data were gridded prior to the generation of section plots and the calculation of mean water-column values (Figs. 2 and 3c, d). The *z*-grid (pressure) bins focused on the upper 1000 m. Python 3.6 Xarray linear method was used as the interpolation scheme.

Nitrate δ^{15}N transported into the Angola Gyre. Cruise A16N sampled both the Equatorial Undercurrent (EUC) and South Equatorial Undercurrent (SEUC) at 0.5°S and 3.6°S, respectively, while the CoFeMUG cruise sampled the South Equatorial Countercurrent (SECC) at 27.5–30°E (Fig. 1 and SI.6). The mean [NO_3^-]-weighted δ^{15}N for the EUC, SEUC, and SECC were estimated to be 5.7‰, 6.0‰ and 6.3‰, respectively. To appropriately weight the nitrate flux of each feeder current, two transport volume scenarios were considered due to the uncertainty in the contribution of the EUC to the Angola Gyre[42]. Scenario A considered the net transport across the northern limb of the Angola Gyre, of 8 Sv, to be apportioned between the SEUC (59%) and the SECC (41%), with no contribution from the EUC[42]. Scenario B considered the net transport across the eastern limb of the Angola Gyre, of 11 Sv, to be apportioned between the SEUC (43%), the SECC (30%), and the EUC (27%)[42]. The mean flux-weighted nitrate δ^{15}N resulting from both transport scenarios was 6.1 ± 0.1‰; this value is used in scenario 2 throughout the study.

Assimilation-corrected, depth-specific fraction of newly fixed nitrate. At the base of the euphotic zone, co-occurring nitrate assimilation and nitrification of

low-$\delta^{15}N$ OM deriving from N_2 fixation raises the $\delta^{15}N$ of nitrate, potentially yielding an underestimation of the depth-specific fraction of newly-fixed nitrate inferred from the $\delta^{15}N$ data (SI.7). During nitrate assimilation, nitrate $\delta^{18}O$ and $\delta^{15}N$ rise in a 1:1 ratio as nitrate consumption proceeds[45,46] while during nitrification, nitrate $\delta^{18}O$ and $\delta^{15}N$ become decoupled[48,102,103]. The nitrate $\delta^{18}O$ data thus reveal (1) the depth at which nitrate assimilation begins to alter to isotopic composition of the nitrate pool and (2) the magnitude of the nitrate assimilation signal, two insights that are not apparent from the nitrate $\delta^{15}N$ data. Assuming that isotopic fractionation associated with nitrate assimilation similarly alters nitrate $\delta^{15}N$ and $\delta^{18}O$ as nitrate consumption proceeds[45,46], we quantified the nitrate assimilation signal at each depth in the water column and subtracted it from the nitrate $\delta^{15}N$ data, beginning at the depth where nitrate $\delta^{18}O$ starts to rise above its mean deep-ocean value. Following the removal of the nitrate assimilation signal, the fraction of newly fixed nitrate at each depth was calculated.

Statistical analyses. To estimate uncertainty on the mean $\delta^{15}N$ of Angola Gyre and western basin nitrate ($\sigma_\theta \leq 27.0$), we calculated the 95% confidence interval associated with a *t*-distribution (for $n < 30$). The same method was adopted to estimate uncertainty on *f* (Eq. 1) for scenarios 1 and 2. To characterize the uncertainty associated with the Angola Gyre N_2 fixation rates, we ran a Monte Carlo simulation of 100k steps assuming a normal probability distribution. We report the standard deviation of the output as the error associated with the rates.

Data availability

Data from the CoFeMUG and A16N cruises can be found in the BCO-DMO database (http://www.bco-dmo.org/dataset/630246/data and http://www.bcodmo.org/dataset/699160/data, respectively). Data from the MET131 cruise can be found in the PANGAEA database (https://doi.org/10.1594/PANGAEA.929671).

Received: 22 November 2021; Accepted: 13 June 2022;
Published online: 30 June 2022

References

1. Smith, S., Phosphorus versus nitrogen limitation in the marine environment. *Limnol. Oceanogr.* **29**, 1149–1160 (1984).
2. Codispoti, L. in *Productivity of the Ocean: Present and Past* (eds Berger, W., Smetacek, V. & Wefer, G.) 377–394 (Wiley, 1989).
3. Broecker, W. & Henderson, G. The sequence of events surrounding Termination II and their implications for the cause of glacial-interglacial CO_2 changes. *Palaeoceanogr. Paleoclimatol.* **13**, 352–364 (1998).
4. Codispoti, L. Is the ocean losing nitrate? *Nature* **376**, 724 (1995).
5. Deutsch, K. et al. Dinitrogen fixation in the World's oceans. *Biogeochemistry* **57**, 47–98 (2002).
6. Deutsch, C., Sarmiento, J., Sigman, D., Gruber, N. & Dunne, J. Spatial coupling of nitrogen inputs and losses in the ocean. *Nature* **445**, 163–167 (2007).
7. Brandes, J. & Devol, A. A global marine-fixed nitrogen isotopic budget: Implications for Holocene nitrogen cycling. *Glob. Biogeochem. Cycles* **16**, 1120 (2002).
8. Garcia, H. E. et al. World Ocean Atlas 2018. Vol 4: Dissolved inorganic nutrients (phosphate, nitrate and nitrate+nitrite, silicate). https://accession.nodc.noaa.gov/NCEI-WOA18 (2018).
9. Moore, C. et al. Large-scale distribution of Atlantic nitrogen fixation controlled by iron availability. *Nat. Geosci.* **2**, 867–871 (2009).
10. Flohr, A., van der Plas, Emeis, K., Mohrholz & Rixen, T. Spatio-temporal patterns of C:N: P ratios in the northern Benguela upwelling system. *Biogeosciences* **11**, 885–897 (2014).
11. Nagel, B. et al. N-cycling and balancing of the N-deficit generated in the oxygen minimum zone over the Namibian shelf — an isotope based approach. *J. Geophys. Res. Biogeosci.* **118**, 1–11 (2013).
12. Coles, V. & Hood, R. Modeling the impact of iron and phosphorus limitations on nitrogen fixation in the Atlantic Ocean. *Biogeosciences* **4**, 455–479 (2007).
13. Wang, W., Moore, K., Martiny, A. & Primeau, F. Convergent estimates of marine nitrogen fixation. *Nature* **566**, 205–211 (2019).
14. Marconi, D. et al. Tropical dominance of N_2 fixation in the North Atlantic Ocean. *Glob. Biogeochem. Cycles* **31**, 1608–1623 (2017).
15. Fonseca-Batista, D. et al. Nitrogen fixation in the eastern Atlantic reaches similar levels in the Southern and Northern Hemisphere. *J. Geophys. Res. Oceans* **122**, 587–601 (2017).
16. Luo, Y. et al. Database of diazotrophs in global ocean: abundance, biomass and nitrogen fixation rates. *Earth Sci. Data* **4**, 47–73 (2012).
17. Snow, J. et al. Environmental controls on the biogeography of diazotrophy and *Trichodesmium* in the Atlantic Ocean. *Glob. Biogeochem. Cycles* **29**, 869–884 (2015).
18. Sohm, J., Webb, E. & Capone, D. Emerging patterns of marine nitrogen fixation. *Nat. Rev. Microbiol.* https://doi.org/10.1038/nrmicro2594 (2011).
19. Browning, T. et al. Nutrient co-limitation at the boundary of an oceanic gyre. *Nat. Lett.* https://doi.org/10.1038/nature24063 (2017).
20. Sarthou, G. et al. Atmospheric iron deposition and sea-surface dissolved iron concentrations in the eastern Atlantic Ocean. *Deep Sea Res. I* **50**, 1339–1352 (2003).
21. Hansell, D., Olson, D., Dentener, F. & Zamora, L. Assessment of excess nitrate development in the subtropical North Atlantic. *Mar. Chem.* **106**, 562–576 (2007).
22. Schlosser, C. et al. Seasonal ITCZ migration dynamically controls the locations of the (sub)tropical Atlantic biogeochemical divide. *Proc. Natl Acad. Sci. USA* **11**, 1438–1442 (2014).
23. Gruber, N. & Sarmiento, J. Global patterns of marine nitrogen fixation and denitrification. *Glob. Biogeochem. Cycles* **11**, 235–266 (1997).
24. Hansell, D., Bates, N. & Olson, D. Excess nitrate and nitrogen fixation in the North Atlantic. *Mar. Chem.* **84**, 243–265 (2004).
25. Weber, T. & Deutsch, C. Oceanic nitrogen reservoir regulated by plankton diversity and ocean circulation. *Nature* **489**, 419–422 (2012).
26. Martiny, A. et al. Strong latitudinal patterns in the elemental ratios of marine plankton and organic matter. *Nat. Geosci.* **6**, 279–283 (2013).
27. Mills, M. & Arrigo, K. Magnitude of oceanic nitrogen fixation influenced by the nutrient uptake ratio of phytoplankton. *Nat. Geosci.* **3**, 412–416 (2010).
28. Knapp, A., DiFiore, P., Deutsch, C. & Sigman, D. Nitrate isotopic composition between Bermuda and Puerto Rico: implications for N_2 fixation in the Atlantic Ocean. *Glob. Biogeochem. Cycles* https://doi.org/10.1029/2007GB003107 (2008).
29. Rafter, P., DiFiore, P. & Sigman, D. Coupled nitrate nitrogen and oxygen isotopes and organic matter remineralization in the Southern and Pacific Oceans. *J. Geophys. Res. Oceans* **118**, 47781–4794 (2013).
30. Minagawa, M. & Wada, E. Nitrogen isotope ratios of red tides organisms in the East China Sea: a characterisation of biological nitrogen fixation. *Mar. Chem.* **19**, 245–259 (1986).
31. Carpenter, E., Harvey, H., Fry, B. & Capone, D. G. Biogeochemical tracers of the marine cyanobacterium *Trichodesmium*. *Deep Sea Res. I* **44**, 27–38 (1997).
32. Knapp, A., Sigman, D. & Lipschultz, F. N isotopic composition of dissolved organic nitrogen and nitrate at the Bermuda Atlantic Time-series Study site. *Glob. Biogeochem. Cycles* https://doi.org/10.1029/2004GB002320 (2005).
33. Sigman, D., Altabet, M., McCorkle, D., Francois, R. & Fischer, G. The delta N-15 of nitrate in the Southern Ocean: nitrogen cycling and circulation in the ocean interior. *J. Geophys. Res.* **105**, 19599–19614 (2000).
34. Noble, A. et al. Basin-scale inputs of cobalt, iron, and manganese from the Benguela-Angola front to the South Atlantic Ocean. *Limnol. Oceanogr.* **57**, 989–1010 (2012).
35. Fripiat, F. et al. Compilation of nitrate d15N in the ocean. PANGAEA. https://doi.org/10.1594/PANGAEA.936484 (2021).
36. Buck, K. & Copley, N. Cobalt, iron and micro-organisms from the upwelling zone to the Gyre (CoFeMUG). BCO-DMO. http://www.bco-dmo.org/dataset/630246/data (2016).
37. Weber, T. & Deutsch, C. Local versus basin-scale limitation of marine nitrogen fixation. *Proc. Natl Acad. Sci. USA* **111**, 8741–8746 (2014).
38. Knapp, A., Casciotti, K., Berelson, W., Prokopenko, M. & Capone, D. Low rates of nitrogen fixation in eastern tropical South Pacific surface waters. *Proc. Natl Acad. Sci. USA* **113**, 4398–4403 (2016).
39. Moroshkin, K., Bubnov, V. & Bulatov, R. Water circulation in the eastern South Atlantic. *Oceanogr. Oceanol.* **10**, 27–34 (1970).
40. Gordon, A. & Bosley, K. Cyclonic gyre in the tropical South Atlantic. *Deep Sea Res.* **38**, S323–S343 (1990).
41. Peterson, R. & Stramma, L. Upper-level circulation in the South Atlantic. *Prog. Oceanogr.* **26**, 1–73 (1991).
42. Mercier, H., Arhan, M. & Lutjeharms, J. Upper-layer circulation in the eastern Equatorial and South Atlantic Ocean in January–March 1995. *Deep Sea Res. I* **50**, 863–887 (2003).
43. Berger, W. Productivity of the Ocean: present and past. Global maps of ocean productivity, W. H. Berger, V. S. Smetacek, and G. Wefer, Eds. Wiley-Interscience, New York, 1989. xviii, 470 pp., illus. $146. Life Sciences Research Reports, vol. 44. From a workshop, Berlin, F.R.G., April 1988. *Science* **247**, 865 (1990).
44. Mohrholz, V., Barthlomomae, C., van der Plas, A. & Lass, H. The seasonal variability of the northern Benguela undercurrent and its relation to the oxygen budget on the shelf. *Continental Shelf Res.* **28**, 424–441 (2008).
45. Granger, J., Sigman, D., Needoba, J. & Harrison, P. Coupled nitrogen and oxygen isotope fractionation of nitrate during assimilation by cultures of marine phytoplankton. *Limnol. Oceanogr.* **49**, 1763–1773 (2004).

46. Granger, J., Sigman, D., Rohde, M., Maldonado, M. & Tortell, P. N and O isotope effects during nitrate assimilation by unicellular prokaryotic and eukaryotic plankton cultures. *Geochim. Cosmochim. Acta* **74**, 1030–1040 (2010).
47. Sarmiento, J., Gruber, N., Brzezinksi, M. & Dunne, J. High-latitude controls of thermocline nutrients and low latitude biological productivity. *Nature* **427**, 56–69 (2004).
48. Sigman, D. et al. The dual isotopes of deep nitrate as a constraint on the cycle and budget of oceanic fixed nitrogen. *Deep Sea Res. I* **56**, 1419–1439 (2009).
49. Marconi, D., Weigand, M. & Sigman, D. Nitrate isotopic gradients in the North Atlantic Ocean and the nitrogen isotopic composition of sinking organic matter. *Deep Sea Res. I* **145**, 109–124 (2019).
50. Lehmann, N. et al. Isotopic evidence for the evolution of subsurface nitrate in the Western Equatorial Pacific. *J. Geophys. Res. Oceans* **123**, 1684–1707 (2018).
51. Altieri, K., Fawcett, S. & Hastings, M. Reactive nitrogen cycling in the atmosphere and ocean. *Annu. Rev. Earth Planet. Sci.* **49**, 523–550 (2021).
52. Baker, A., Lesworth, T., Adams, C., Jickells, T. & Ganzeveld, L. Estimation of atmospheric nutrient inputs to the Atlantic Ocean from 50°N to 50°S based on large-scale field sampling: fixed nitrogen and dry deposition of phosphorus. *Glob. Biogeochem. Cycles* https://doi.org/10.1029/2009GB003634 (2010).
53. Sohm, J. et al. Nitrogen fixation in the South Atlantic Gyre and the Benguela Upwelling System. *Geophys. Res. Lett.* https://doi.org/10.1029/2011GL048315 (2011b).
54. Subramaniam, A., Mahaffey, C., Johns, W. & Mahowald, N. Equatorial upwelling enhances nitrogen fixation in the Atlantic Ocean. *J. Geophys. Res. Lett.* **40**, 1766–1771 (2013).
55. Staal, M., Meysman, F. & Stal, L. Temperature excludes N_2-fixing heterocystous cyanobacteria in the tropical oceans. *Nature* **425**, 504–507 (2003).
56. An, C. Atlantic Ocean phytoplankton south of the Gulf of Guinea on profiles along 11 and 14 degrees S. *Oceanology* **6**, 896–901 (1971).
57. Foster, R., Subramaniam, A. & Zehr, J. Distribution and activity of diazotrophs in the Eastern Equatorial Atlantic. *Environ. Microbiol.* **11**, 741–750 (2009).
58. Vieira, L. et al. Unprecedented Fe delivery from the Congo River margin to the South Atlantic Gyre. *Nat. Commun.* **11**, 556 (2020).
59. Scholz, F., McManus, J., Mix, A., Hensen, C. & Schneider, R. The impact of ocean deoxygenation on iron release from continental margin sediments. *Nat. Geosci. Lett.* https://doi.org/10.1038/NGEO2162 (2014).
60. Conway, T. & John, S. Quantification of dissolved iron sources to the North Atlantic Ocean. *Nature* https://doi.org/10.1038/nature13482 (2014).
61. Tagliabue, A. et al. How well do global ocean biogeochemistry models simulate dissolved iron distributions? *Glob. Biogeochem. Cycles* https://doi.org/10.1002/2015GB005289 (2016).
62. Homoky, W. et al. Iron colloids dominate sedimentary supply to the ocean interior. *Proc. Natl Acad. Sci. USA* https://doi.org/10.1073/pnas.2016078118 (2021).
63. Lima, C., Mendes, C., Tavano, V., Detoni, A. & Secchi, E. Chemotaxonomy-based mapping of phytoplankton communities in the subtropical Southwestern Atlantic Ocean, with emphasis on the marine cyanobacterium *Trichodesmium*. *Prog. Oceanogr.* **172**, 77–88 (2019).
64. Tuerena, R. et al. Nutrient cycling in the Atlantic basin: the evolution of nitrate isotope signatures in water masses. *Glob. Biogeochem. Cycles* **29**, 1830–1844 (2015).
65. Benavides, M. & Voss, M. Five decades of N_2 fixation research in the North Atlantic Ocean. *Front. Mar. Sci.* https://doi.org/10.3389/fmars.2015.00040 (2015).
66. Marconi, D. et al. Nitrate isotope distributions on the US GEOTRACES North Atlantic cross-basin section: signals of polar nitrate sources and low latitude nitrogen cycling. *Mar. Chem.* **177**, 143–156 (2015).
67. Pinedo-González, P. et al. Surface distribution of dissolved trace metals in the oligotrophic ocean and their influence on phytoplankton biomass and productivity. *Glob. Biogeochem. Cycles* **29**, 1763–1781 (2015).
68. Moffett, J. & German, C. Distribution of iron in the Western Indian Ocean and the Eastern tropical South pacific: an inter-basin comparison. *Chem. Geol.* https://doi.org/10.1016/j.chemgeo.2019.119334 (2020).
69. Rafter, P., Sigman, D., Charles, C., Kaiser, J. & Haug, G. Subsurface tropical Pacific nitrogen isotopic composition of nitrate: Biogeochemical signals and their transport. *Glob. Biogeochem. Cycles* https://doi.org/10.1029/2010GB003979 (2012).
70. Capone, D. et al. An extensive bloom of the N2-fixing cyanobacterium *Trichodesmium erythraeum* in the central Arabian Sea. *Mar. Ecol. Prog. Ser.* **172**, 281–292 (1998).
71. Bange, H., Rixen, T., Johansen, A. & Siefert, R. First direct measurements of N2 fixation during a Trichodesmium bloom in the eastern Arabian Sea. *Glob. Biogeochem. Cycles* **14**, 1283–1297 (2000).
72. Gandhi, N. et al. First direct measurements of N2 fixation during a *Trichodesmium* bloom in the eastern Arabian Sea. *Glob. Biogeochem. Cycles* https://doi.org/10.1029/2010GB003970 (2011).
73. Jayakumar, A. et al. Biological nitrogen fixation in the oxygen-minimum region of the eastern tropical North Pacific ocean. *ISME J.* https://doi.org/10.1038/ismej.2017.97 (2017).
74. White, A. et al. Nitrogen fixation in the Gulf of California and the Eastern Tropical North Pacific. *Prog. Oceanogr.* https://doi.org/10.1016/j.pocean.2012.09.002 (2013).
75. Fernandez, C., Farías, L. & Ulloa, O. Nitrogen fixation in denitrified marine waters. *PLoS ONE* https://doi.org/10.1371/journal.pone.0020539 (2011).
76. Moutin, T. et al. Phosphate availability and the ultimate control of new nitrogen input by nitrogen fixation in the tropical Pacific Ocean. *Biogeosciences* https://doi.org/10.5194/bg-5-95-2008 (2008).
77. Dekaezemacker, J. et al. Evidence of active dinitrogen fixation in surface waters of the eastern tropical South Pacific during El Niño and La Niña events and evaluation of its potential nutrient controls. *Glob. Biogeochem. Cycles* https://doi.org/10.1002/gbc.20063 (2013).
78. Landolfi, A., Kähler, P., Koeve, W. & Oschlies, A. Global marine N_2 fixation estimates: from observations to models. *Front. Microbiol.* https://doi.org/10.3389/fmicb.2018.02112 (2018).
79. Brandes, J., Devol, A., Yoshinari, T., Jayakumar, D. & Naqvi, S. Isotopic composition of nitrate in the central Arabian Sea and eastern tropical North Pacific: a tracer for mixing and nitrogen cycles. *Limnol. Oceanogr.* **43**, 1680–1689 (1998).
80. Sigman, D. et al. Coupled nitrogen and oxygen isotope measurements of nitrate along the eastern North Pacific margin. *Glob. Biogeochem. Cycles* https://doi.org/10.1029/2005GB002458 (2005).
81. Casciotti, K., Buchwald, C. & McIlvin, M. Implications of nitrate and nitrite isotopic measurements for the mechanisms of nitrogen cycling in the Peru oxygen deficient zone. *Deep Sea Res. I* https://doi.org/10.1016/j.dsr.2013.05.017 (2013).
82. Buchwald, C., Santoro, A., Stanley, R. & Casciotti, K. Nitrogen cycling in the secondary nitrite maximum of the eastern tropical North Pacific off Costa Rica. *Glob. Biogeochem. Cycles* https://doi.org/10.1002/2015GB005187 (2015).
83. Casciotti, K. & McIlvin, M. Isotopic analyses of nitrate and nitrite from reference mixtures and application to Eastern Tropical North Pacific waters. *Mar. Chem.* https://doi.org/10.1016/j.marchem.2007.06.021 (2007).
84. Peng, X. et al. Ammonia and nitrite oxidation in the Eastern Tropical North Pacific. *Glob. Biogeochem. Cycles* https://doi.org/10.1002/2015GB005278 (2015).
85. Redfield, A., Ketchum, B. & Richards, F. in *The Composition of Sea-Water Comparative and Descriptive Oceanography* (ed. Hill, M. N.) 26–77 (Interscience Publishers, 1963).
86. Kuypers, M. et al. Massive nitrogen loss from the Benguela upwelling system through anaerobic ammonium oxidation. *Proc. Natl Acad. Sci. USA* https://doi.org/10.1073/pnas.0502088102 (2005).
87. Stramma, L., Johnson, G., Sprintall, J. & Mohrholz, V. Expanding oxygen-minimum zones in the tropical oceans. *Science* **320**, 655–658 (2008).
88. Hamilton, D. et al. Impact of changes to the atmospheric soluble iron deposition flux on ocean biogeochemical cycles in the Anthropocene. *Glob. Biogeochem. Cycles* https://doi.org/10.1029/2019GB006448 (2020).
89. Letscher, R., Hansell, D., Carlson, C., Lumpkin, R. & Knapp, A. Dissolved organic nitrogen in the global surface ocean: distribution and fate. *Glob. Biogeochem. Cycles* **27**, 141–153 (2013).
90. Dyhrman, S. et al. Phosphonate utilization by the globally important marine diazotroph *Trichodesmium*. *Nature* https://doi.org/10.1038/nature04203 (2006).
91. Sohm, J. & Capone, D. Phosphorus dynamics of the tropical and subtropical north Atlantic: *Trichodesmium* spp. versus bulk plankton. *Mar. Ecol. Prog. Ser.* https://doi.org/10.3354/meps317021 (2006).
92. Letscher, R., Moore, J., Teng, J. & Primeau, F. Variable C: N: P stoichiometry of dissolved organic matter cycling in the Community Earth System Model. *Biogeosciences* **12**, 209–221 (2015).
93. Martiny, A. et al. Biogeochemical controls of surface ocean phosphate. *Sci. Adv.* **5**, eaax0341 (2019).
94. Becker, S. et al. GO-SHIP repeat hydrography nutrient manual: the precise and accurate determination of dissolved inorganic nutrients in seawater, using continuous flow analysis methods. *Front. Mar. Sci. Methods* https://doi.org/10.3389/fmars.2020.581790 (2020).
95. Sigman, D. et al. A bacterial method for the nitrogen isotopic analysis of nitrate in seawater and freshwater. *Anal. Chem.* **73**, 4145–4153 (2001).
96. Casciotti, K., Sigman, D., Hastings, M., Bohlke, J. & Hilkert, A. Measurement of the oxygen isotopic composition of nitrate in seawater and freshwater using the denitrifier method. *Anal. Chem.* **74**, 4905–4912 (2002).
97. Firing, E. & Hummon, J. M. Shipboard ADCP Measurements. In *The GO-SHIP Repeat Hydrography Manual: A Collection of Expert Reports and Guidelines*. Version 1, (eds Hood, E. M., Sabine C. L. & Sloyan, B. M.). 11pp. (IOCCP Report Number 14; ICPO Publication Series Number 134). https://doi.org/10.25607/OBP-1352 (2010).
98. Grasshoff, K., Kremling, K. & Ehrhardt, M. in *Verlag Chemie* (eds Grasshoff, K., Ehrhardt, K. & Kremling, K.) 419 (Wiley-VCH, 1999).
99. Granger, J. & Sigman, D. Removal of nitrite with sulfamic acid for nitrate N and O isotope analysis with the denitrifier method. *Rapid Commun. Mass Spectrom.* **23**, 3753–3762 (2009).

100. Gonfiantini, R. Stable isotope reference samples for geochemical and hydrological investigations. *Int. J. Appl. Radiat. Isotopes* https://doi.org/10.1016/0020-708X(84)90059-0 (1984).
101. Böhlke, J., Mroczkowski S. J. & Coplen, T. Oxygen isotopes in nitrate: new reference materials for 18O:17O:16O measurements and observations on nitrate-water equilibration. *Rapid Commun. Mass Spectrom*. https://doi.org/10.1002/rcm.1123 (2003).
102. Buchwald, C., Santoro, A., McIlvin, M. & Casciotti, K. Oxygen isotopic composition of nitrate and nitrite produced by nitrifying cocultures and natural marine assemblages. *Limnol. Oceanogr*. **57**, 1361–1375 (2012).
103. Boshers, D., Granger, J., Tobias, C., Bohlke, J. & Smith, R. Constraining the oxygen isotopic composition of nitrate produced by nitrification. *Environ. Sci. Technol*. https://doi.org/10.1021/acs.est.8b03386 (2019).

Acknowledgements

We thank the captains and crew of the R/V *Knorr*, R/V *Meteor* and R/V *Ronald H. Brown*, as well as cruise participants E. Vorrath and C. Frame, and lab technician M. Ankele. This work was supported by the South African National Research Foundation (114673 and 130826 to T.M., 115335, 116142 and 129320 to S.E.F.); the US National Science Foundation (CAREER award, OCE-1554474 to J.G., OCE-1736652 to D.M.S. and K.L.C., OCE-05-26277 to K.L.C.); the German Federal Agency for Education and Research (DAAD-SPACES 57371082 to T.M.); the Royal Society (FLAIR fellowship to S.E.F.); and the University of Cape Town (T.M., J.G., S.E.F.). The authors also recognize the support of the South African Department of Science and Innovation's Bio-geochemistry Research Infrastructure Platform (BIOGRIP).

Author contributions

T.M., M.R.M. and D.M. made the nitrate isotope measurements. M.A.S. and A.E.N. collected and measured the CoFeMUG cruise iron samples. K.L.C., K.D. and D.M.S. supported the nitrate isotope analyses in their laboratories. D.M., D.M.S. and K.-C.E. provided data and samples. T.M., J.G., D.M.S. and S.E.F. led the data interpretation. All authors contributed to the paper, led by T.M., with major contributions from J.G., D.M.S. and S.E.F. All authors approved the final submission.

Competing interests

The authors declare no competing interests.

Additional information

Supplementary information The online version contains supplementary material available at https://doi.org/10.1038/s43247-022-00474-x.

Correspondence and requests for materials should be addressed to Tanya Marshall.

Peer review information *Communications Earth & Environment* thanks Sarah Reynolds, Robyn Tuerena and the other anonymous reviewer(s) for their contribution to the peer review of this work. Primary handling editors: Clare Davis, Heike Langenberg. Peer reviewer reports are available.

Reprints and permission information is available at http://www.nature.com/reprints

Publisher's note Springer Nature remains neutral with regard to jurisdictional claims in published maps and institutional affiliations.

Open Access This article is licensed under a Creative Commons Attribution 4.0 International License, which permits use, sharing, adaptation, distribution and reproduction in any medium or format, as long as you give appropriate credit to the original author(s) and the source, provide a link to the Creative Commons license, and indicate if changes were made. The images or other third party material in this article are included in the article's Creative Commons license, unless indicated otherwise in a credit line to the material. If material is not included in the article's Creative Commons license and your intended use is not permitted by statutory regulation or exceeds the permitted use, you will need to obtain permission directly from the copyright holder. To view a copy of this license, visit http://creativecommons.org/licenses/by/4.0/.

© The Author(s) 2022